AD-A173 659 ELECTRICAL STIMULATION OF CELLULAR RESPONSE- RESPONSES AND MECHANISMS(U) MASSACHUSETTS INST OF TECH CAMBRIDGE DEPT OF ELECTRICAL ENGIN R C LEE ET AL 01 OCT 86 1/1

UNCLASSIFIED N00014-85-K-0153 F/G 6/3 NL

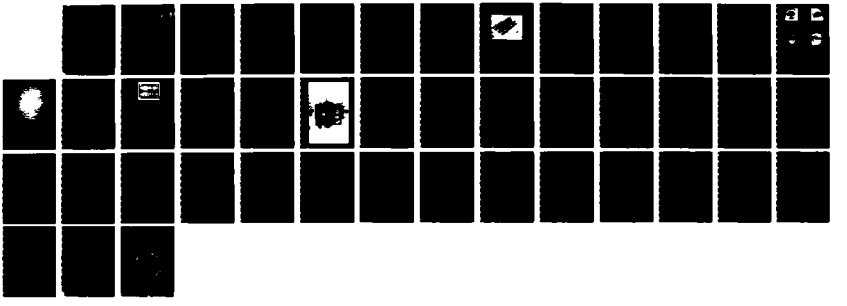

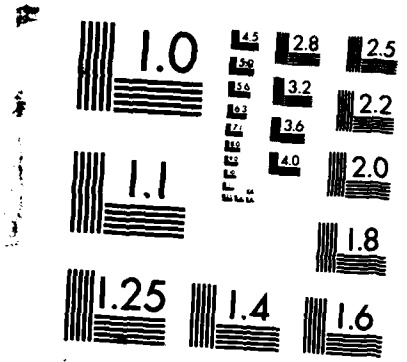

CONTINUUM ELECTROMECHANICS GROUP
LABORATORY FOR ELECTROMAGNETIC AND ELECTRONIC SYSTEMS
DEPARTMENT OF ELECTRICAL ENGINEERING AND COMPUTER SCIENCE
MASSACHUSETTS INSTITUTE OF TECHNOLOGY

ANNUAL PROJECT REPORT

ELECTRICAL STIMULATION OF CELLULAR RESPONSE: RESPONSES AND MECHANISMS

OCTOBER 1, 1986

Raphael C. Lee, M.D., Sc.D., Principal Investigator
John R. Kenny, S.B., Graduate Research Assistant
Russell M. Basch, S.B., Graduate Research Assistant
Bradford I. Tropea, Undergraduate Research Assistant

(U)

SECURITY CLASSIFICATION OF THIS PAGE

REPORT DOCUMENTATION PAGE

1a. REPORT SECURITY CLASSIFICATION (U)	1b RESTRICTIVE MARKINGS NA
2a. SECURITY CLASSIFICATION AUTHORITY NA	3. DISTRIBUTION/AVAILABILITY OF REPORT Distribution Unlimited
2b DECLASSIFICATION/DOWNGRADING SCHEDULE NA	
4 PERFORMING ORGANIZATION REPORT NUMBER(S)	5. MONITORING ORGANIZATION REPORT NUMBER(S) NA
6a NAME OF PERFORMING ORGANIZATION Massachusetts Institute of Technology 6b. OFFICE SYMBOL (If applicable) NA	7a. NAME OF MONITORING ORGANIZATION Office of Naval Research
6c. ADDRESS (City, State, and ZIP Code) Dept. of Electrical Engineering & Computer Science 38-377 Cambridge, MA 02139	7b. ADDRESS (City, State, and ZIP Code) 800 North Quincy Street Arlington, VA 22217-5000
8a. NAME OF FUNDING/SPONSORING ORGANIZATION Office of Naval Research 8b. OFFICE SYMBOL (If applicable)	9. PROCUREMENT INSTRUMENT IDENTIFICATION NUMBER N00014-85-K-0153
8c. ADDRESS (City, State, and ZIP Code) 800 North Quincy Street Arlington VA 22217-5000	10. SOURCE OF FUNDING NUMBERS PROGRAM ELEMENT NO. 61153N; PROJECT NO. RR04108; TASK NO. NR 441; WORK UNIT ACCESSION NO.

11. TITLE (Include Security Classification)

Electrical Stimulation of Cellular Responses: Responses and Mechanisms

12. PERSONAL AUTHOR(S)

R. C. Lee, John R. Kenny, Russell M. Basch, Bradford I. Tropea

13a. TYPE OF REPORT	13b. TIME COVERED	14. DATE OF REPORT (Year, Month, Day)	15. PAGE COUNT
Annual	FROM 1/15/85 TO 1/14/86	86-10-1	40

16 SUPPLEMENTARY NOTATION

17 COSATI CODES			18. SUBJECT TERMS (Continue on reverse if necessary and identify by block number)
FIELD	GROUP	SUB-GROUP	

19 ABSTRACT (Continue on reverse if necessary and identify by block number)

With an in-vitro system which minimized the sample-to-sample variation by using an isogenetic cell population at a uniform cell density, we observed that:

(1) Bovine (and Human) fibroblasts and bovine chondrocytes respond to low frequency sinusoidal electric current by altering the rate of biosynthesis of extracellular matrix structural macromolecules. This effect was dependent on stimulus frequency and amplitude. (2) The sensitivity of the fibroblasts to the fields was found to depend on the orientation of the cells in the direction of the field. Cells oriented such that their major axis was aligned in the direction of the electric field responded to weaker electric currents than those aligned perpendicular to the field. This evidence is consistent with the hypothesis that the mechanism of electrochemical transduction involves a change in the transmembrane potential. (3) We have also observed that while chondrocytes in organ culture do not change their biosynthetic behavior in response to

20 DISTRIBUTION/AVAILABILITY OF ABSTRACT ☐ UNCLASSIFIED/UNLIMITED ☐ SAME AS RPT ☐ DTIC USERS	21. ABSTRACT SECURITY CLASSIFICATION
22a NAME OF RESPONSIBLE INDIVIDUAL Dr. Charles N. Rafferty	22b TELEPHONE (Include Area Code) / 22c. OFFICE SYMBOL

DD FORM 1473, 84 MAR 83 APR edition may be used until exhausted. All other editions are obsolete

SECURITY CLASSIFICATION OF THIS PAGE

10Hz a.c. current densities up to 1 ma/cm^2, chondrocytes in hydrated collagen gels respond to current densities as low as 50 μa/cm^2 Hz. This suggests that either the enzymatic digestion process alters the behavior of cells or the interaction of the cells with the extracellular matrix modulates the response.

As we have demonstrated a decrease in protein synthesis, one is left to question why the cell reduces its protein synthesis, and if another cell function has been enhanced. Studies on the synthesis of glycosaminoglycans by chondrocytes in hydrated gels suggest that GAG production is also depressed. We have recently begun to utilize DNA staining techniques with flow cytometric measurements to investigate mitotic activity in the presence of very low frequency electric fields.

Other research being examined is the altering of protein secretion rate of cells by modulations of exocytosis. Under the guidance of Dr. David Albertini (consultant), we have established an experimental method and performed initial measurements of the rate of transport of membrane vesicles within bovine fascia and human dermal fibroblasts. The vesicles are labeled with Lucifer Yellow CH (1 mg/ml) which is incorporated into the vesicles during serum stimulated liquid phase endocytosis. Thus far, only a few experiments have been done and no difference in the rates of transport of vesicles has been detected.

Efforts are well underway to establish a real-time fluorescent assay of intracellular NAD(P)H levels. In theory, changes in cytoplasmic NAD(P) H levels should be correlated to changes in the rate of protein biosynthesis. Therefore, as proposed this technique should enable us to sense changes in cellular biosynthesis in real time. With the radiolabeled precursor incorporation studies as the benchmark, we plan to extend the frequency-amplitude threshold response determinations to finely delineate the cutoff frequencies using this new method. This should provide invaluable information regarding the kinetics of the electrochemical transductive coupling at the plasma membrane.

Thus far, the installation of the vibration isolation table, pulsed nitrogen laser, inverted microscope, emission spectrometer, dual channel boxcar integrator and other equipment needed to measure the emitted fluorescent light from a single cell excited at 340 nm (near UV) wavelength has been completed. Calibration using buffered solutions of NADH (Sigma Chem) has been performed.

Finally, efforts have been undertaken to determine the relationship between an applied source and the electric field generated between two electrodes. The rectification and harmonic distortion with respect to a pure sinusoid that occur when voltage and current sources are applied across the electrodes have and are being quantified and explained.

I. SYNOPSIS

Project objectives for the first year include:

1. Define the relationship between physiologic electrical currents and the rate of biosynthesis of extracellular matrix proteins by bovine fibroblasts and chondrocytes.
2. Determine the extent of cellular proliferative response to the same physiologically relevant electrical stimulus.
3. Set up and calibrate a real-time fluorometric assay of intracellular NAD(P)H using microfluorometric techniques.

I.a Relevance

The long term goals of this project are: (1) to determine which cellular biochemical processes are modulated by physiologic electric fields, (2) to determine the physiochemical transduction mechanisms which couple extracellular fields to intracellular events, and (3) to explore the usefulness of electric stimuli as a control of synthetic tissue growth and development.

Our primary working hypothesis is that many mammalian non-excitable cell types are sensitive to naturally occurring interstitial electrical currents which arise from in-vivo sources and that cells use these signals to establish and maintain the structural integrity of their environment. Evidence supporting this concept is substantial. Furthermore, we find it plausible that electric stimuli may be useful to regulate generation of living tissue substitutes, modulation of normal wound healing and perhaps in the management of hypertropic disorders of wound healing. We believe these goals to be consistent with the mission of the Office of Naval Research.

I.b Summary

With an in-vitro system which minimized the sample-to-sample variation by using a isogenetic cell population at a uniform cell density, we observed that:

1. Bovine (and Human) fibroblasts and bovine chondrocytes respond to low frequency sinusoidal electric current by altering the rate of biosynthesis of extracellular matrix structural macromolecules. This effect was dependent on stimulus frequency and amplitude.

2. The sensitivity of the fibroblasts to the fields was found to depend on the orientation of the cells in the direction of the field. Cells oriented such that their major axis was aligned in the direction of the electric field responded to weaker electric currents than those aligned perpendicular to the field. This evidence is consistent with the hypothesis that the mechanism of electrochemical transduction involves a change in the transmembrane potential.

3. We have also observed that while chondrocytes in organ culture do not change their biosynthetic behavior in response to 10 Hz a.c. current densities up to 1 ma/cm^2, chondrocytes in hydrated collagen gels respond to current densities as low as 50 μa/cm^2 at 20 Hz. This suggests that either

the enzymatic digestion process alters the behavior of cells or the interaction of the cells with the extracellular matrix modulates the response.

As we have demonstrated a decrease in protein synthesis, one is left to question why the cell reduces its protein synthesis, and if another cell function has been enhanced. Studies on the synthesis of glycosaminoglycans by chondrocytes in hydrated gels suggest that GAG production is also depressed. We have recently begun to utilize DNA staining techniques with flow cytometric measurements to investigate mitotic activity in the presence of very low frequency electric fields.

Other research being examined is the altering of protein secretion rate of cells by modulations of exocytosis. Under the guidance of Dr. David Albertini (consultant), we have established an experimental method and performed initial measurements of the rate of transport of membrane vesicles within bovine fascia and human dermal fibroblasts. The vesicles are labeled with Lucifer Yellow CH (1 mg/ml) which is incorporated into the vesicles during serum stimulated liquid phase endocytosis. Thus far, only a few experiments have been done and no difference in the rates of transport of vesicles has been detected.

Efforts are well underway to establish a real-time fluorescent assay of intracellular NAD(P)H levels. In theory, changes in cytoplasmic NAD(P)H levels should be correlated to changes in the rate of protein biosynthesis. Therefore, as proposed this technique should enable us to sense changes in cellular biosynthesis in real time. With the radiolabeled precursor incorporation studies as the benchmark, we plan to extend the frequency-amplitude threshold response determinations to finely delineate the cutoff frequencies using this new method. This should provide invaluable information regarding the kinetics of the electrochemical transductive coupling at the plasma membrane.

Thus far, the installation of the vibration isolation table, pulsed nitrogen laser, inverted microscope, emission spectrometer, dual channel boxcar integrator and other equipment needed to measure the emitted fluorescent light from a single cell excited at 340 nm (near UV) wavelength has been completed. Calibration using buffered solutions of NADH (Sigma Chem.) has been performed.

Finally, efforts have been undertaken to determine the relationship between an applied source and the electric field generated between two electrodes. The rectification and harmonic distortion with respect to a pure sinusoid that occur when voltage and current sources are applied across the electrodes have and are being quantified and explained.

II. BIOSYNTHETIC RESPONSES

II.a Introduction

The role of physiologic electric fields in the regulation of tissue growth, remodeling, and repair present questions of burgeoning interest to biologists and clinicians. We studied the sensitivity of mammalian fibroblasts to electric currents using neonatal bovine fibroblasts in collagen gels. The frequency and intensity dependence of electric field

modulation of proline incorporation into extracellular and intracellular protein was measured over the frequency range of 0.1 Hz to 1 kHz. A frequency and amplitude dependent reduction in the rate of incorporation was observed. Using tissues containing cells aligned either parallel or perpendicular to the electric field, it was observed that this response was dependent on the orientation of the cells relative to the direction of the applied electric field.

Determination of cell sensitivity to electric fields which span the physiologic frequency range would allow an assessment of the extent to which physiologic fields could regulate cellular processes. Comparison of frequency dependence with the kinetics of known cellular processes may provide insight to the putative mechanisms of energy transduction.

II.b Methods

Connective tissue remodeling is known to be regulated by physical stresses [1]. Since fibroblasts are primarily responsible for this remodeling activity, these cells were selected for use in this study. Neonatal bovine fibroblasts were obtained by disaggregating superficial fascial tissue from the thigh of 2 week old calves by serial trypsin and collagenase digestions. The cells obtained were plated in flasks, maintained in Dulbecco's Modified Eagle's medium (DME) containing 10% calf serum and passed 2 to 5 times prior to incorporation into gels.

The behavior of many, if not all cell types, is strongly influenced by the cells' environment. So, to maximize control over extracellular matrix composition and cell density, we chose to fabricate tissues of constant composition by *incorporating* fibroblasts in collagen matrices (FPCM). To fabricate the fibroblast populated collagen matrices (FPCM), bovine fibroblasts were incorporated into 2 mg/ml type I collagen gels using the technique reported by Bell et al. [2]. Native collagen was obtained through 0.5M acetic acid extraction of the tail tendons of young (less than 2 month old) Sprague-Dawley rats. The soluble collagen solution was stored in sterile 0.1M acetic acid at 4 ^{o}C until needed. At the time of gel casting neutralized collagen solution and cells suspended in media were mixed and warmed to 37 ^{o}C. Gelation occurred within 10 minutes and within several hours the gel was visibly contracting. Three days after gel casting both matrix contraction and cell population doubling were found to plateau and the FPCM were strong enough to be handled. Hematoxylin and eosin (H&E) staining of 10 micron thick histologic sections [McLeod, submitted] revealed a randomly oriented FPCM with cell and matrix densities similar to that of loose connective tissue. Cells in these FPCM stopped proliferating prior to contact inhibition and cell density approximated loose connective tissue [2]. The electrical conductivity of the FPCM was found to be less than 10% different from the surrounding media. On the third day after casting, 1 cm^2 samples were cut from the FPCM and randomly assigned to control or exposure groups.

Control and exposure samples were mounted in teflon holders which had circular apertures, and then, mounted in a teflon chamber (Fig. 1) containing fresh serum-free media supplemented with 10 µCi/ml ^{3}H-proline and 1 millimolar proline. The chambers were incubated in 95% air-5% CO_2 mixture at 37 ^{o}C and 99% humidity. A programmable current source provided stable low frequency currents with d.c. flow limited to less than 0.1% of

the a.c. amplitude. Current was passed through the exposure samples for 12 hours via platinum electrodes which were separated from the bath by media bridges and convection barriers (membranes). Current density was determined by dividing the total current by the aperture area of the holders, and field intensity in the FPCM samples was estimated using Ohm's Law and the value of the media resistivity.

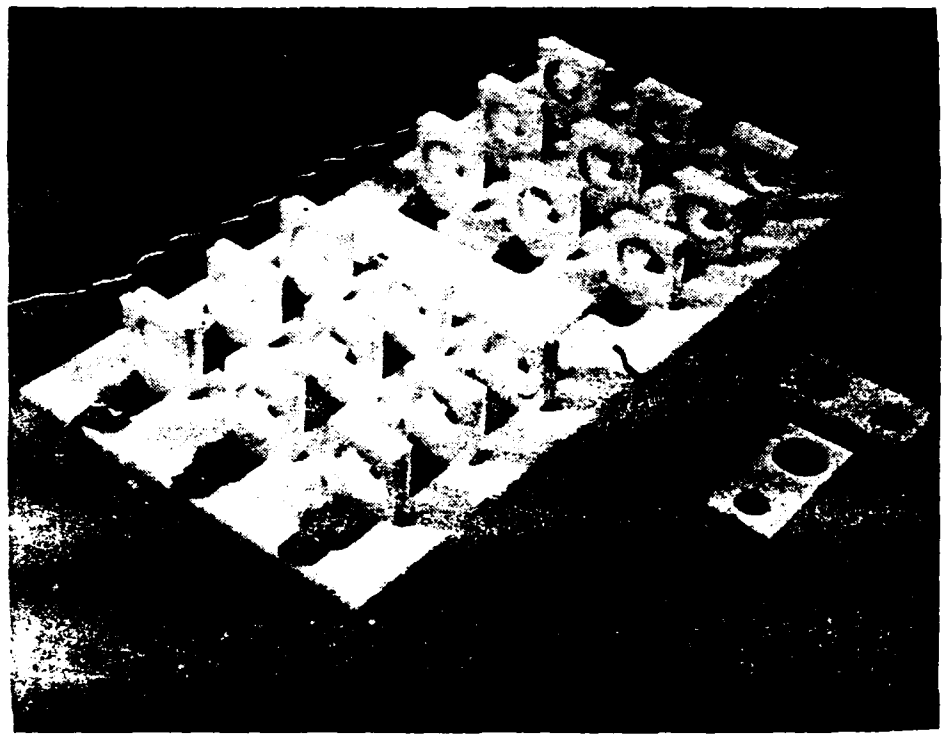

Figure 1: Experimental apparatus used to expose random FPCM samples to electrical fields. Platinum electrodes are separated from the site of the tissue sample via media bridges. A programmable current source with series d.c. blocking capacitors maintains a constant current within the chamber media, independent of variations in electrode-electrolyte interfacial impedance. The lumen of the sample holder establishes a defined current density, and therefore field intensity, through the FPCM

Accumulation of newly synthesized protein was estimated by measuring the incorporation of proline into macromolecules. Immediately after a 12 hour exposure period, samples were washed at 4 °C, then digested with bacterial collagenase, after which the cells were separated from the matrix components by centrifugation. After counting the cells, cell were disrupted [3] and intracellular protein precipitated with cold trichloroacetic acid. Scintillation counts of both the matrix and cell fractions were obtained and normalized to cell number. Control studies demonstrated an incorporation rate of 450 picomoles or proline per hour per million cells in serum-free medium, addition of 10% calf serum increased this synthesis rate by a factor of 1.7-2.0. Collagen, assayed by differential salt precipitation [4], accounted for approximately 4% of recovered protein synthesized [5] which is consistent with a previous report [6].

Experiments were performed over a range of current densities (0.1 $\mu a/cm^2$ to 1 ma/cm^2, r.m.s.) and frequencies (0.1 to 1000 Hz). The observed response to electrical current was an alteration in the rate of incorporation of ^3H-proline into secreted protein. Figure 2a exhibits the response as a function of current density at 1 Hz and shows that currents as low as 1 $\mu A/cm^2$ cause a 30% reduction in the incorporation of newly synthesized protein into the extracellular matrix. Above this current density, increasing the current over two orders of magnitude does not significantly increase the response. However halving the current density leads to no response. The transition is described as a threshold because the response is strongly field intensity dependent for only a very small fraction of the total range of intensities which we found capable of evoking the response. The threshold current density was found to be frequency specific.

The frequency dependence of the response plotted in Figure 2(b) suggests a frequency range which may be optimally effective for alteration of extracellular matrix protein synthesis. This observation is summarized in Figure 2c where the effect of both frequency and current density are plotted over the range of 1-1000 Hz and 0.1 to 100 $\mu A/cm^2$ respectively. Peak sensitivity was recorded at 10 Hz where a current density of only 0.5 $\mu A/cm^2$ produced a significant reduction in protein incorporation in the matrix component. Since the media resistivity was 65 Ω-cm [7], this corresponds to a peak field intensity in the medium of 45 $\mu V/cm$. The incorporation of radiolabel into intracellular protein was found to reflect the pattern seen in the extracellular matrix.

To test the possibility that chemical by-products of electrolysis were responsible for the response, experiments were performed in which 100 $\mu a/cm^2$ was passed through the media for 12 hours, then discontinued immediately prior to transfer of the FPCM to the chambers. The FPCM were then kept in the chambers for 12 hours while bathed in the electrically conditioned media for 12 hours then analyzed as usual. No significant difference in rates of proline incorporation was observed between the control samples and samples which had been in the electrically preconditioned media. This suggested that the responses measured required direct exposure to the electric field and the electric field effects were not mediated by stable non-volatile by-products of electrolysis. Similarly, to test whether the cellular responses were a consequence of thermal effects, the magnitude of the Joule heating was analyzed. The temperature rise of the media adjacent to the sample position was measured as a function of both current density and time. It was found that a current

density of 10 ma/cm^2 was required to produce a steady state temperature increase of 0.5^{o}C with an onset time constant approximately equal to 20 minutes [7]. The steady state temperature elevation was proportional to the current density squared. For the range of current densities used in the actual experiments, the expected temperature rise was much less than 0.1^{o}C, which is less than the temperature oscillations in the incubators.

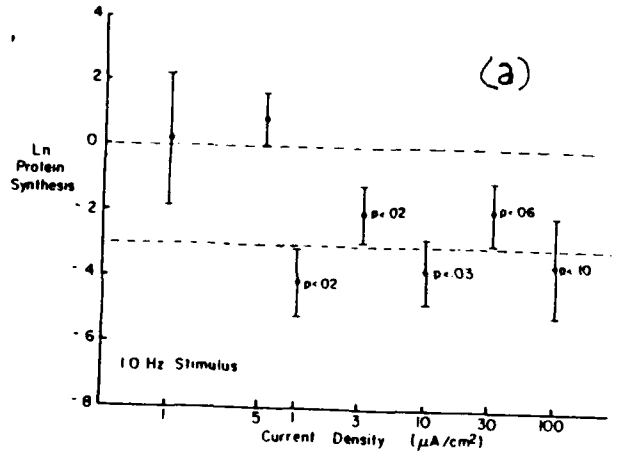

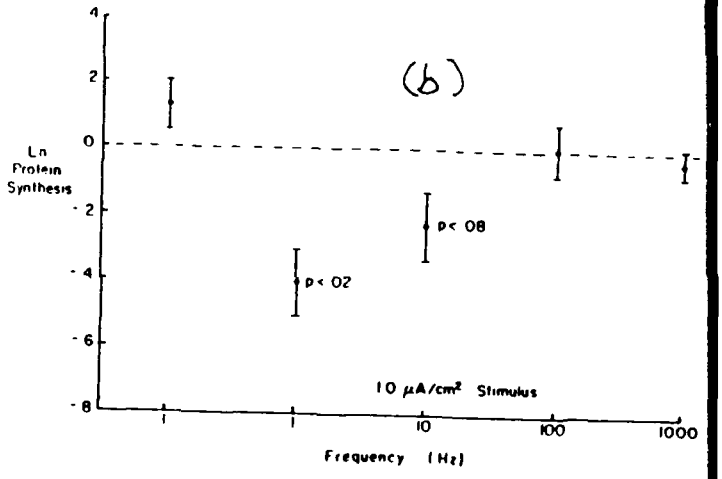

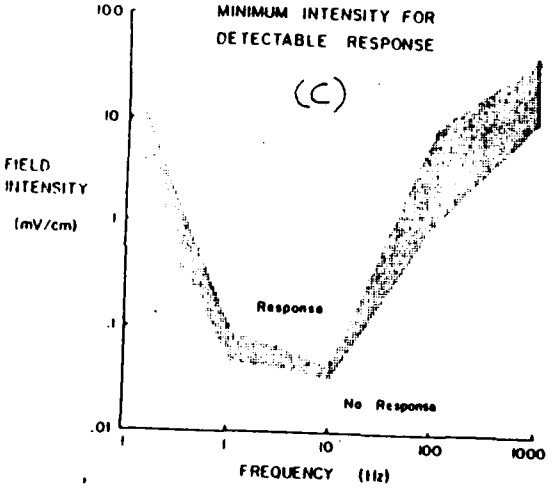

Figure 2: Response of bovine fibroblasts in FPCM to 12 hour exposures to low frequency electric fields, at 37°C, in serumless Dulbecco's media. ^{3}H-proline incorporation (cpm) were normalized to cell count for each sample. The incorporation ratio of experimental to control samples was determined and the natural logarithm (Ln) is statistically analyzed. The mean and standard error of the mean for n samples ($6 < n < 20$) are plotted. "p" value indicates probability of log normalized data differing from 0.0 as determined by the non-parametric Dixon - Mood sign test. (a) Extracellular proline accumulation vs. current density at 1 Hz. stimulus frequency. (b) Normalized extracellular proline accumulation vs. frequency for 1 μA/cm². (c) Minimum field intensity for a detectable response. Summary of results for all tested frequencies and current densities. Current densities converted to peak field intensities using the measured media resistivity of 65 Ω-cm. The lower boundary of the gray region represents the highest field intensity at which no significant change in extracellular protein accumulation was detected, the upper boundary represents the lowest intensity evoking a significant change.

II.c Dependence on Cell Orientation

For the frequencies used in these experiments, plasma membrane impedance is many orders of magnitude higher than that of the cytoplasm. When a cell the size of a bovine fibroblast is placed in an applied field, the membrane essentially prevents current flow through the cell. Current exclusion results in an additional voltage drop across the cell membrane which is spatially distributed over the cell surface [8]. This distribution is a function of cell geometry, such that for any point on the membrane the induced perturbation of the membrane potential is proportional to $E_o L/2$, where E_o is the applied field magnitude, and L the maximum linear dimension of the cell in the direction of the field. For non-spherical cells, a maximum perturbation of the membrane potential will occur when the major axis of the cell is aligned in the direction of the imposed electric field. The importance of the cell membrane potential in regulating cellular activity suggests that this alteration in transmembrane potential may mediate the cellular response to low frequency extracellular electric fields.

One test of this hypothesis makes use of the nonspherical shape of the cells used in this study. Fibroblasts, in the collagen lattices, took on the bipolar morphology which has been previously described [9]. The maximum length of these cells was approximately 150 μm, which is 7-10 times longer than their minor dimension. If the depression in incorporation is mediated by a membrane potential change, then cells exposed to fields parallel to their major axis should exhibit a lower threshold intensity than cells with their major axis perpendicular to the applied electric field. Of course other, probably significant, parameter changes occur with changes in the cells' orientation. The plasma membrane area over which the maximum transmembrane potential alteration occurs is reduced when cells are aligned with the field. Also, the interaction between the cell surface and the tangent electric field will depend on cell orientation. Therefore, interpretation of orientation dependence may be complicated. Nonetheless, such an effect would provide further evidence that the response is dependent only on the electric field.

We investigated the role of cell orientation by constructing FPCM with cells predominantly oriented in one direction. To uniformly align cells in the collagen matrix, the FPCMs were allowed to contract over 3 days around two porous polyethylene posts held at a fixed separation distance of two centimeters (Figure 3). The FPCM contracted with the cells and collagen aligned along an axis defined by the line passing through the porous posts at opposite ends of the petri dish (Figure 4). The electrical conductivity of the media filled posts were within 10% of free media solution.

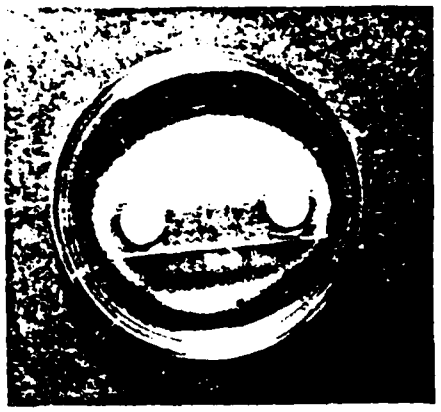

A

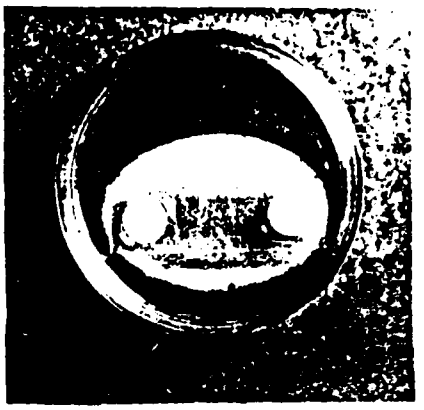

B

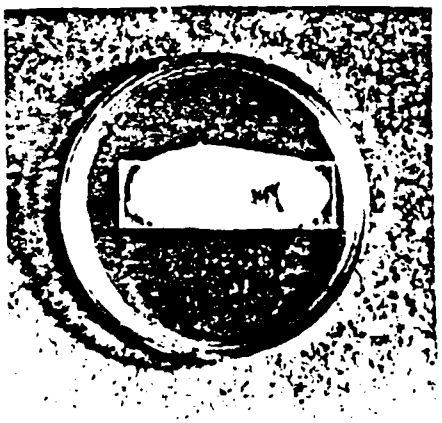

C

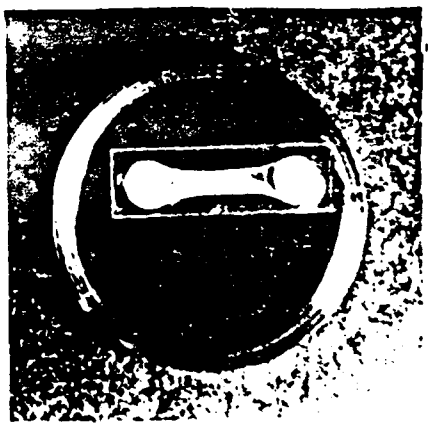

D

Figure 3: Contraction nad formation of oriented FPCM. Fibroblast populated gels cast into 60 mm petri dishes with two polyethylene posts held at a fixed separation. (a) Hydrated gel after 12 hours of contraction; (b) 24 hours; (c) 48 hours; and (d) 72 hours, the condition at which the oriented FPCMs were utilized.

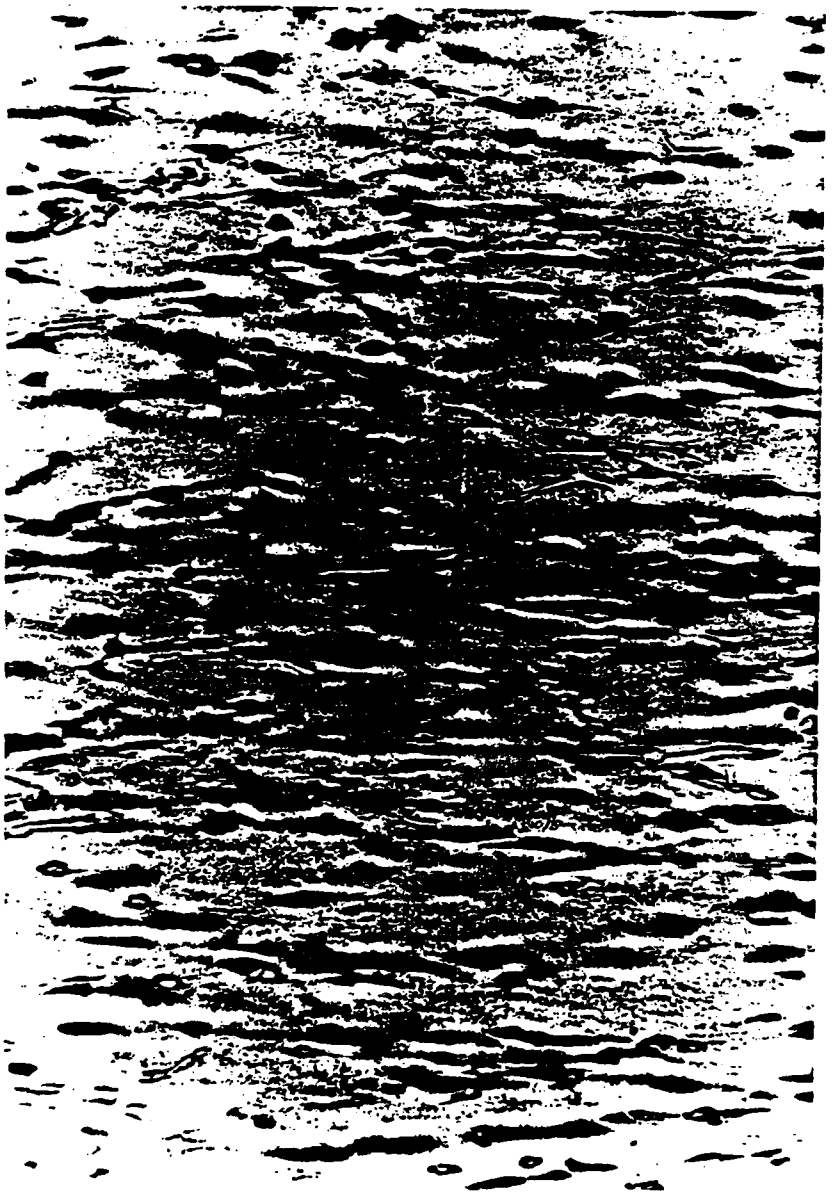

Figure 4: Bovine fibroblasts in oriented FPCM as seen by bright-field microscopy 18 hours post casting. Vertical axis of photo is longitudinal axis between fixed polyethylene posts of orientation apparatus.

Three days after casting, the FPCM were placed in the exposure chamber shown in Figure 5. In each chamber, half of the FPCM were installed with the major axis of the cells parallel to the applied electric field, while the other half were installed with cells oriented perpendicular to the direction of the electric field. Current was passed through the experimental samples for 12 hours. Following the exposure period, the center section between the posts were removed and analyzed for proline incorporation using the same protocol as used for the FPCM with random cell orientation.

Since the cells were most sensitive to 10 Hz fields, this frequency was chosen to examine the effect of orientation on the field intensity threshold. For the randomly oriented FPCM, a current density of 0.3 $\mu A/cm^2$ produced no significant effect on the rate of proline incorporation. Whereas, when cells aligned with the electric field were exposed to the same current density a significant reduction in proline incorporation was detected. By contrast, the cells oriented perpendicular to the field did not respond. As illustrated in Figure 6, cell alignment with respect to the electric field modulates the intensity threshold. Cells parallel to the field respond at 0.3 $\mu A/cm^2$, while cells perpendicular to the field have still not shown a significant depression in protein secretion at 0.6 $\mu A/cm^2$. At 10 Hz, the cells with their major axis aligned with the field detect a field intensity of 45 $\mu V/cm$. This corresponds to a maximum membrane potential perturbation of less than 0.5 μV.

II.d Discussion of Biosynthetic studies

This study has demonstrated that protein production in FPCM is more sensitive to electric fields over the physiologic frequency range than previously shown for connective tissue cells. If the same level of sensitivity exists in-vivo it seems possible that mechanically induced fields in connective tissue are capable of triggering cell mediated changes in tissue composition. Similarly, fibroblasts in-vivo may be sensitive to electric fields from other sources, depending on its intensity and frequency.

These experiments further demonstrate that the orientation of the cells with respect to the imposed electric field affects the ability of the cells to respond. This result is consistent with the possibility of the cells detecting a transmembrane potential perturbation, but it is not conclusive. Since the FPCM oriented parallel and perpendicular to the field were in the same bathing media, these studies strongly suggest that the response was due exclusively to the imposed electric fields, and not a secondary factor such as heating, media contamination, mechanical vibration, or ambient magnetic fields within the incubators.

The frequency dependence of the response suggests two modes of electrically mediated control of tissue composition. At constant frequency, a biosynthetic response could follow an increase in local current density. Alternately, if a change in loading rate leads to a change in the frequency, then this could also lead to a response. Through either pathway, the fields might be used as a feedback signal for tissue remodeling and repair [10].

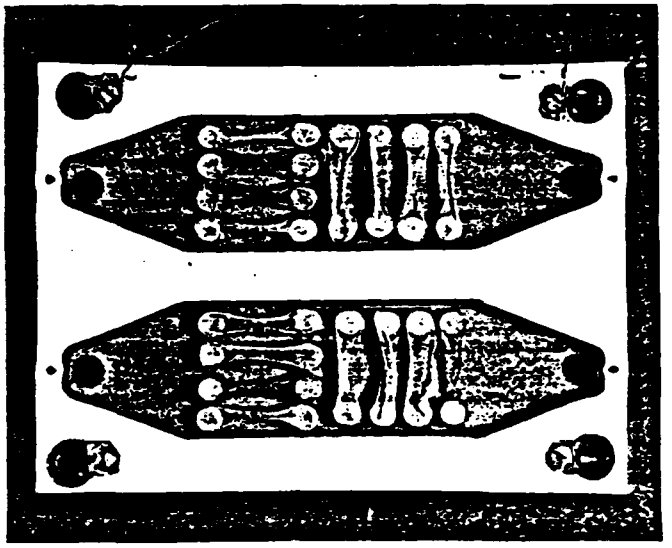

Figure 5: Exposure chamber for oriented FPCM samples. Each chamber holds four samples with cells oriented parallel with the applied field, and four perpendicular to the applied field. Current density is dictated by media depth for a constant current source.

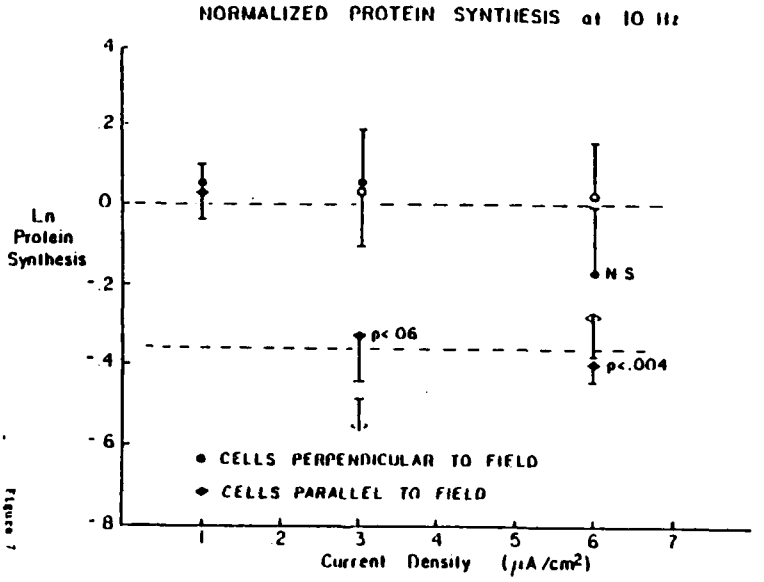

Figure 6: Normalized extracellular proline incorporation (closed symbols) and intracellular proline incorporation (open symbols) vs. current density for oriented FPCMs at 10 Hz. Samples with cells oriented parallel to field demonstrate a threshold current density below that seen in the samples of randomly oriented cells, while samples with cells perpendicular show no depression of proline incorporation at a current intensity above the threshold level for randomly oriented samples. Data points are the mean and standard error of the mean.

The molecular mechanisms through which weak electric fields trigger a biosynthetic response are unknown. Since a variety of cell types, including the special electroreceptors of aquatic animals [11], also exhibit extreme sensitivity to electric fields, we suggest that this capability is very primative and serves a fundamental role in the interaction of living systems with their environment.

III. PINOCYTOTIC VESICLE TRANSPORT

III.a Introduction

We have recently demonstrated that physiologically relevant electric fields (those of low magnitude and frequency) affected the ability of bovine fibroblasts to incorporate ^{3}H-proline into protein. Secretion is the final step in the production of extracellular macromolecules. Since secretion of macromolecules is partly mediated by exocytosis, it is plausible that electric fields might affect the rate of biosynthesis through the alteration of intracellular transport of membrane vesicles.

To explore this possibility we have undertaken a three phase project. The first part was the development of a real time technique for measuring membrane transport. The second phase was developing a theoretical framework for interpreting membrane transport data. These have been completed. The final stage, which is currently being pursued, is the use of the real time technique, and the use of fixed cells to determine the potential relationship between a field and transport. In this report we will summarize the conclusions of the first two stages of this effort.

III.b Background

Traditionally, the three membrane transport processes, intracellular, exocytosis, and endocytosis, are monitored using fixed cells. The cells are allowed to utilize labeled vesicles for various amounts of time and then are fixed. After fixation all of the measurements are made.

Fixation has many nice features. Sterile technique is not required after fixation. Because the cells do not have to observed during the experiment, a large number of cells can be tested at one time, and because it is so widely used, it is the most readily comparable form of data.

What data from fixed cells lack, though, is the insight a real time approach gives. In real time an individual cell is traced through time; it is monitored while it is alive. So a visual picture of evolution over time of an effect on a single cell is developed. To get such a picture with fixation, one must superimpose the reactions of many different cells. This leaves the distinct possibility that the general idea might get lost in the noise of individual cellular differences. For this reason, it was decided to develop a real-time technique to measure the effect of an electric field on membrane transport.

III.c Method

The protocol for tracking membrane transport in real time was as follows:

Bovine or Human Fibroblasts (depending on the choice of experiment) of passage number five or less were plated onto sterile microscope cover glass (25mm by 25mm) and maintained in Dulbecco's Modified Media (Gibco) with 10% calf serum. The cells were kept in incubators at 37oC and with 5% CO_2. Twenty-four hours before the experiment was to take place the media was changed to D.M.E.M. without calf serum. The cells were labeled for forty minutes with 1 mg/ml Lucifer Yellow CH (Molecular Probes). The cells were washed five times with Hanks w/out Calcium and Magnesium (Gibco) and were then given a final wash with Hanks w/ Calcium and Magnesium (Gibco) to remove any phenol red that attached. After the washing, the cover glass with the fibroblasts was placed over a 1.5cm diameter hole in the custom built chamber shown in Figure 7. The glass slip was affixed to the teflon chamber by a thin layer of Bacitracin Ointment U.S.P. (fougera). The chamber was then filled with Hanks with Calcium and Magnesium.

Transport was observed by putting the chamber on the stage of a Nikon Diaphot microscope. The dye was excited by a 100W Osram Mercury Arc Lamp that was filtered by the Nikon "B" filter block. A Nikon FT 35mm camera was attached to the microscope and pictures were taken in 15 minute intervals. A neutral density filter (90% intensity attenuation) was placed in front of the arc lamp, and that light path was shut off between pictures to minimize bleaching.

Proper temperature was maintained by the Nikon Incubator NP-2 attached to the microscope stage. Dehydration was avoided by using tissue culture plastic to cover the chamber. The electric field was applied by using an I.E.C. F34 function generator with a Kepco amplifier. A 100Ω resistor was attached between the generator and the chamber. The voltage across the resistor was then measured with a Tektronix 2215 60MHz oscilloscope, and current was determined. The field intensity was then calculated.

Ten minutes after labeling was finished, the electric field was turned on, and transport was monitored for two hours. Under the same conditions a control experiment was also run. Pictures were taken ten minutes after labeling for two hours in fifteen minute intervals.

III.d A Theoretical Framework for Interpreting Membrane Transport Data

To analyze any changes that are seen when monitoring membrane transport, one must understand the potential mechanisms by which the field could affect a cell. There are three main possibilities:

1) The field's impact could be indirect. By changing the transmembrane potential and surface charge distribution, the transport of ions across the membrane could be affected. This could trigger a biochemical reaction that might alter rate of membrane pinching and fusion or the rate of vesicle transport.

2) The field could have a direct effect. Pinocytotic vesicles have a fixed surface charge and therefore will electrophoresis in an electric field. This could alter transport, since the distance between the vesicles and the cell membrane influences the probability of fusion.

3) Or it could be a combination of the above.

To understand these possible mechanisms, and which one is the dominant cause, an expression for the electrophoretic velocity of a vesicle

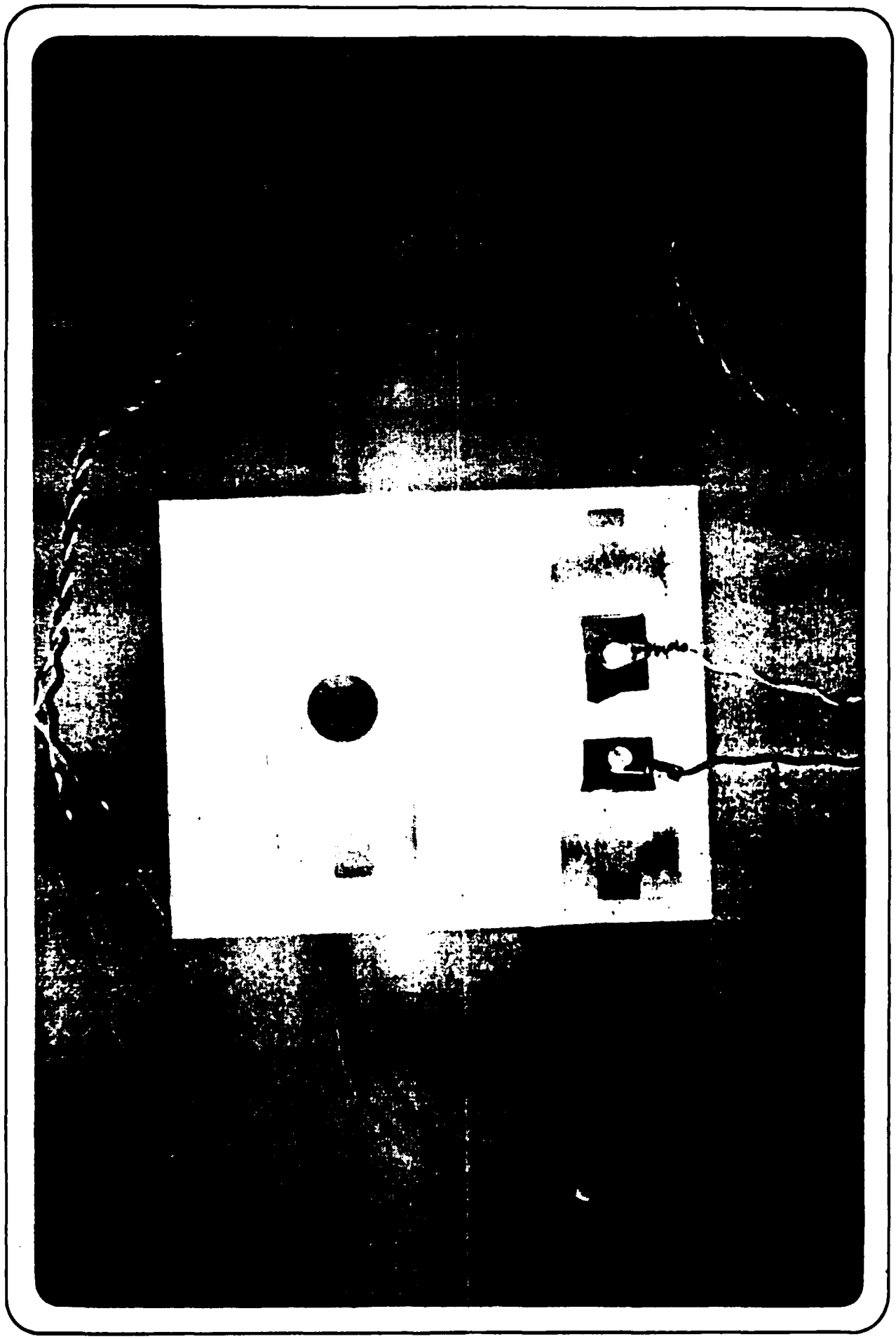

Figure 7

inside a cell was needed.

III.e Derivation of an Electrophoretic Velocity Equation

Steady state electrophoretic movement is due to the balance between viscous and electrical forces. This results in the velocity of a particle being proportional to the strength of the imposed electric field.

Neglecting the redistribution of the fixed membrane charges due to the electric field, there are two characteristics of pinocytotic vesicles that can be used to arrive at an electrophoretic velocity expression. First, since the double layer for a pinocytotic vesicle is estimated at 1nm, while its diameter ranges from 40nm - 500nm (depending on the cell type), it can be concluded that the electrical double layer is very thin compared to the dimensions of our colloid (pinocytotic vesicle). Second, since the pinocytotic vesicle's membrane has a much lower conductivity than that of the cytoplasm, the colloid can be considered insulating. Since its surface conductance is low, the distribution of the intracellular electric field is, therefore, practically unaffected by the vesicle.

Under those conditions, neglecting relaxation, electrophoretic velocity can be expressed as [13]:

$$V_e = \frac{\varepsilon \zeta E_c}{4\pi\eta}$$

where η is the viscosity coefficient of the intracellular fluid. This constant is unknown, but it is known that it must be less than or equal to that of water which is $1.002 \cdot 10^{-3}$ kg/sec-m

ε is the cytoplasm's dielectric constant, again approximately that of water -- $80\varepsilon_o$ -- $7.08 \cdot 10^{-10}$(F/m)

ζ is the zeta potential, which is defined as the electrical potential in the slipping plane between the fixed and flowing liquid of the planar model used to derive our expression. It is approximately 26mv.

E_c is the cytoplasmic field.

Therefore,

$$V_e = 1.46 \cdot 10^{-9}(As^2/kg) \cdot E_c$$

The problem then is to determine E_c.

III.f Determining The Cytoplasmic Electric Field Using a DC Spherical Model

A DC spherical model can often provide insight into the magnitude of the intracellular fields and membrane voltage drops induced by a low frequency stimulus. For the conditions of this project such a model, shown in Figure 8, would contain the following parameters:

R_c -- the radius at which the cytoplasm and the membrane meet -- 30μm [14]

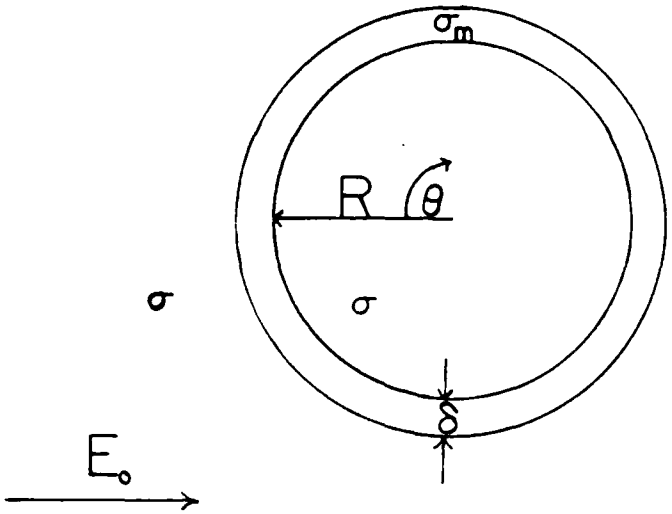

Figure 8

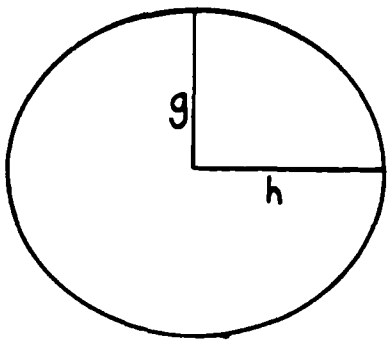

Figure 9

g=a and h=b

or

g=b and h=a

R_e -- the radius at which the membrane and the external media touch -- 30.01μm

δ -- the membrane thickness ($R_e - R_c$) -- 10nm

σ_c , σ_m, σ_e -- the conductivities of the cytoplasm, membrane, and external media -- 1 , 10^{-8} to 10^{-6}, and 1 mho/m, respectively

ε_c, ε_m, ε_e -- the dielectric constants of the cytoplasm, membrane, and external media -- $7.08 \cdot 10^{-10}$, $1.77 \cdot 10^{-11}$, and $7.08 \cdot 10^{-10}$ F/m, respectively

For simplicity it is assumed that each of these constants is uniform within each region, and that unpaired charges occur solely at the regional boundaries.

Since this is a dc analysis, Faraday's Law is expressed as:

$$\nabla \times E = -\frac{\partial \mu H}{\partial t} = 0$$

The electric field, thus, is uniquely represented by a scalar potential that must obey Possoin's equation:

$$\nabla^2 \phi = -\frac{\rho}{\varepsilon}$$

since there are free charges only at boundaries, in each region this expression reduces to Laplace's equation:

$$\nabla^2 \phi = 0$$

Membrane transport experiments take place over hours. Since the charge relaxation time for these materials is so fast, dc steady state conditions prevail. From charge conservation:

$$\nabla \cdot J + \frac{\partial \rho}{\partial t} = 0 = \nabla \cdot J$$

Since charge transport is dominated by Ohmic conduction:

$$n \cdot (\sigma_1 E_1 - \sigma_2 E_2) = 0$$

$$\sigma_e E_{1r}(r = R_e) = \sigma_m E_{2r}(r = R_e)$$

$$\sigma_m E_{2r}(r = R_c) = \sigma_c E_{3r}(r = R_c)$$

and since these fields are conservative:

$$\phi_1(r = R_e) = \phi_2(r = R_e)$$

$$\phi_2(r = R_c) = \phi_3(r = R_c)$$

These boundary conditions yield the following four expressions:

$$-E_o R_e + \frac{\phi_e}{R_e^2} = -\phi_{m1} R_e + \frac{\phi_{m2}}{R_e^2}$$

$$\sigma_m(\phi_{m1} + \frac{2\phi_{m2}}{R_e^3}) = \sigma_e(E_o + \frac{2\phi_e}{R_e^3})$$

$$-\phi_{m1} R_c + \frac{\phi_{m2}}{R_c^2} = -\phi_c R_c$$

$$\sigma_m(\phi_{m1} + \frac{2\phi_{m2}}{R_c^3}) = \sigma_c \phi_c$$

Therefore:

$$\Delta v_m = -\frac{\delta^3 R_c(15\sigma\sigma_m + 12\sigma^2) + \delta^2 R_c^2(9\sigma\sigma_m + 18\sigma^2) + \delta^4(6\sigma\sigma_m + 3\sigma^2) + 9\delta R_c^3\sigma^2}{(3\delta R_c^2 + 3\delta^2 R_c + \delta^3)(2\sigma_m^2 + 5\sigma\sigma_m + 2\sigma^2) + 9R_c^3\sigma\sigma_m} E_o\cos\theta$$

This can be reduced. $A\sigma^2 + B\sigma\sigma_m + C\sigma_m^2 \approx A\sigma^2$ if the first term is much larger than the other two, i.e. $\frac{A\sigma^2}{B\sigma\sigma_m} >> 1$ and $\frac{A\sigma^2}{C\sigma_m^2} >> 1$.

Equivalently, $\frac{A}{B} >> \frac{\sigma_m}{\sigma}$ and $\frac{C}{A} >> (\frac{\sigma_m}{\sigma})^2$. Because of the low membrane conductivity this is in fact the case. Therefore:

$$\Delta v_m = -\frac{12\delta^3 R_c\sigma^2 + 18\delta^2 R_c^2\sigma^2 + 3\delta^4\sigma^2 + 9\delta R_c^3\sigma^2}{(6\delta R_c^2 + 6\delta^2 R_c + 2\delta^3)\sigma^2 + 9R_c^3\sigma\sigma_m} E_o\cos\theta$$

Likewise, an expression of the form $AR_c^3 + BR_c^2\delta + CR_c\delta^2 + D\delta^3$ can be simplified to AR_c^3 if its first term is much larger than the others, i.e. $\frac{A}{B} >> \frac{\delta}{R_c}$, $\frac{A}{C} >> (\frac{\delta}{R_c})^2$, and $\frac{A}{D} >> (\frac{\delta}{R_c})^3$. Due to the small membrane width this is true for cells. Therefore:

$$\Delta v_m \approx -\frac{9\delta R_c^3\sigma^2}{6\delta R_c^2\sigma^2 + 9R_c^3\sigma\sigma_m} E_o\cos\theta$$

$$\rightarrow \Delta v_m = -\frac{3\delta R_c \sigma}{2\delta\sigma + 3R_c\sigma_m} E_o \cos\theta$$

Normalizing each term in this expression gives:

$$\Delta v_m = -\frac{3\delta}{2\frac{\delta}{R_c} + 3\frac{\sigma_m}{\sigma}} E_o \cos\theta$$

Thus if $\frac{\delta}{R_c} >> \frac{\sigma_m}{\sigma}$ then

$$\Delta v_m = -\frac{3}{2} R_c E_o \cos\theta$$

If $\frac{\delta}{R_c} << \frac{\sigma_m}{\sigma}$ then

$$\Delta v_m = -\delta\frac{\sigma}{\sigma_m} E_o \cos\theta$$

Likewise the solution for ΔE_c is:

$$\Delta E_c = \frac{(9R_c^3 + 27\delta R_c^2 + 9\delta^2 R_c + 9\delta^3)\,\sigma\sigma_m}{(3\delta R_c^2 + 3\delta^2 R_c + \delta^3)(2\sigma_m^2 + 5\sigma\sigma_m + 2\sigma^2) + 9R_c^3\sigma\sigma_m} E_o \cos\theta$$

Making the same approximations gives:

$$\Delta E_c = \frac{3R_c\sigma_m}{2\delta\sigma + 3R_c\sigma_m} E_o \cos\theta$$

$$\Delta E_c = \frac{1}{\frac{2\delta\sigma}{3R_c\sigma_m} + 1} E_o \cos\theta$$

Plugging in the numbers gives:

$$\Delta E_c = .00448\ E_o \cos\theta \text{ for } \sigma_m = 10^{-6} \text{ mho/m}$$

$$\Delta E_c = 4.48 \cdot 10^{-5} E_o \cos\theta \text{ for } \sigma_m = 10^{-8} \text{ mho/m}$$

Therefore, a 225 mv/m source would induce an internal field less than or equal to 1 mv/m.

The expression for this upper bound of electrophoretic velocity becomes:

$$V_e \leq 6.54 \cdot 10^{-12}(As^2/kg)\, E_o \cos\theta$$

For a 225 mv/m source the induced electrophoretic velocity would be:

$$V_e \leq 1.47 \cdot 10^{-12}\ (As^2V/kg)$$

III.g The Electrophoretic Velocity using an AC Spherical Cell Model

A slightly more accurate model can be derived when the alternating nature of the exciting fields is accounted for. As long as the exciting source remains within the electrostatic domain, [15] if a spherical cell were to be exited by a single frequency source, all of the geometric boundary conditions would remain the same. Laplace's solution would have the same form, but the two time dependent conditions derived from charge conservation would be modified:

$$\nabla \cdot J + \frac{\partial}{\partial t}\nabla \cdot D = 0$$

At the spherical boundaries:

$$\sigma_1 E_r^{\ 1} - \sigma_2 E_r^{\ 2} + \frac{\partial}{\partial t}(\varepsilon_1 E^1_{\ r} - \varepsilon_2 E^2_{\ r}) = 0$$

With cosinusoidal input these boundary conditions become in phasor form:

$$(\sigma_1 + j\omega\varepsilon_1)E_{1r} = (\sigma_2 + j\omega\varepsilon_2)E_{2r}$$

$$(\sigma_e + j\omega\varepsilon_e)E_{1r}(r = R_e) = (\sigma_m + j\omega\varepsilon_m)E_{2r}(r = R_e)$$

$$(\sigma_m + j\omega\varepsilon_m)E_{2r}(r = R_c) = (\sigma_c + j\omega\varepsilon_c)E_{3r}(r = R_c)$$

The only difference, thus, between the ac solutions and the dc counterpart is that σ_x is replaced by $\sigma_x + j\omega\varepsilon_x$. Their solution, therefore, is the same as the dc solution with σ_x replaced with $\sigma_x + j\omega\varepsilon_x$. The approximated forms of these equations are:

$$\Delta v_m \approx -\frac{3\delta R_c(\sigma + j\omega\varepsilon)}{2\delta(\sigma + j\omega\varepsilon) + 3R_c(\sigma_m + j\omega\varepsilon_m)} E_o \cos\theta$$

$$\Delta E_c \approx \frac{3R_c(\sigma_m + j\omega\varepsilon_m)}{2\delta(\sigma + j\omega\varepsilon) + 3R_c(\sigma_m + j\omega\varepsilon_m)} E_o \cos\theta$$

Rearrangement yields:

$$\Delta v_m \approx -\frac{3\delta R_c}{2\delta + 3R_c\dfrac{(\sigma_m + j\omega\varepsilon_m)}{(\sigma + j\omega\varepsilon)}} E_o \cos\theta$$

$$\Delta E_c \approx \frac{1}{\dfrac{2\delta\ (\sigma + j\omega\varepsilon)}{3R_c(\sigma_m + j\omega\varepsilon_m)} + 1} E_o \cos\theta$$

Since $\frac{\varepsilon_m}{\sigma_m} >> \frac{\varepsilon}{\sigma}$, with respect to frequency, the largest internal field and the smallest membrane voltage drop will occur at the largest experimental frequency using this model. Our experiments have ranged up to 100Hz. In which case

$$\Delta E_c = .00448\ E_o \cos\theta \text{ for } \sigma_m = 10^{-6} \text{ mho/m}$$

$$\Delta E_c = 4.48 \cdot 10^{-5} E_o \cos\theta \text{ for } \sigma_m = 10^{-8} \text{ mho/m}$$

For frequencies at 100Hz and below, both the ac and dc expressions yield the same numerical results for three significant digits. So the same electrophoretic velocity as well would be obtained.

III.h Upperbound for Electrophoretic Velocity of a Cell of an Arbitrary Elliptical Geometry

When viewing transport data, although instructive, a spherical model for a cell is clearly not accurate. Fibroblasts growing in monolayer lie very close to the glass plane, while they can reach up to 2.5mm in the other directions. From observations it is clear that an ellipsoidal model would be more appropriate. But these generalized spheroids do not allow a separation of variables for Laplace's equation, and therefore they can not be solved analytically. [8] On the other hand they can not simply be ignored since most data indicates that for a given length in the direction of the electric field the intracellular field is lowest with a sphere. [16] So the electrophoretic effects that are not possible in the sphere could conceivably occur with a more oblate or prolate model. We have, thus, developed an expression for the upper bound for an intracellular electric field in a convex geometry. Note: this expression should only be used as an upper bound. Due to the difficulties with the geometry, it is undoubtedly considerably higher than the real field. But such a calculation has its purposes.

Intracellular electric fields for generalized geometries can not be solved exactly, but if the voltage drop at all points on the cell membrane is known, the current through any region of the membrane would be known:

$$i = \int_m \frac{v_m(u_1,u_2)\sigma_m}{\delta_d}\, du_1 du_2$$

A closed contour at a constant value for one of the ellipsoid's principal axes, call it A, is a two dimensional shell (ellipse or a circle depending on the axis). By charge conservation, the total amount of current flowing through the membrane on either side of A must equal the total amount of current flowing the planar surface bounded by A.

$$i_A = i_{A'} = i_{A''}$$

where i_A = the current flowing through the planar surface bounded by A, $i_{A'}$ = the current flowing through the smaller region of the membrane bounded by

bounded by A. Using Ohm's Law and uniform conductivity:

$$i_A = \int J dS_A = \sigma_c \int E \cdot dS_A = \sigma_c \int \frac{E \cdot dS_A}{S_A} S_A = \sigma_c E_{avA} S_A$$

where E_{avA} is the average value of the normal component to the planar surface of A of the intracellular electric field. and S_a is the Surface area of the planar region bounded by A.

$$E_{avA} = \frac{i_A}{\sigma_c S_a} = \frac{i_{(A')}}{\sigma_c S_a}$$

$$i_{A'} = \int_m \frac{\sigma_c v_m}{\delta_d} dS_m \leq \frac{\sigma_m V_{max}}{\delta_d} S_m$$

Where S_m is the surface area of the smaller portion of membrane bounded by the contour A.

$$\rightarrow E_{avA} \leq \frac{\sigma_m v_{max} S_m}{\sigma_c \delta_d S_a} = D$$

So for any given planar contour there is a bound, D, for the maximum component of the electric field perpendicular to the plane. To find the bound for the maximum component of an electric field within the cell, the contour in which D is maximized must be found. That contour is the contour which maximizes S_m/S_a.

III.h.1 An Upper Bound for S_m/S_a

As shown in Figure 9, a general spheroidal geometry can be expressed as:

$$\frac{x^2}{a^2} + \frac{y^2}{a^2} + \frac{z^2}{b^2} = 1$$

By symmetry the bound for a contour at x=f will equal the bound for a contour at y=f. So there are two independent regions where this problem must be solved (Figure 10). First for z=c $c \geq 0$ = z@-c: the above expression yields a contour a which is a circle with radius:

$$r_o = a\left(1 - \frac{c^2}{b^2}\right)$$

$$\rightarrow S_A = \pi a^2 \left(1 - \frac{c^2}{b^2}\right)$$

S_m is less than the surface area for an open cylinder of length b - c and radius r_o:

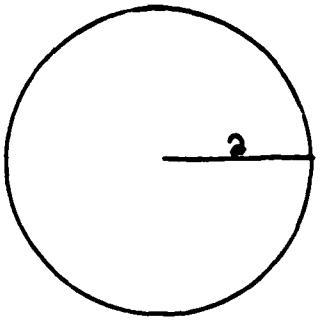

z=c

or

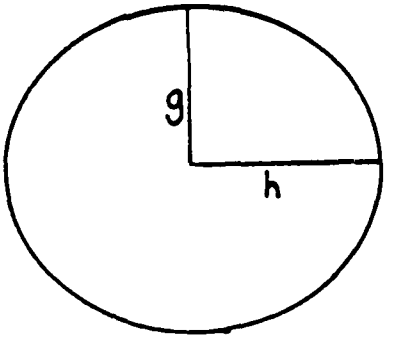

x=f

Figure 10

g=a and h=b

or

g=b and h=a

$$S_m < \pi a^2 \left(1 - \frac{c^2}{b^2}\right) + 2\pi a \left(1 - \frac{c^2}{b^2}\right)^{\frac{1}{2}}(b - c)$$

$$\rightarrow \frac{S_m}{S_a} < 1 + \frac{2(b - c)}{a \left(1 - \frac{c^2}{b^2}\right)^{\frac{1}{2}}}$$

Call this bound, F. F's extremum with respect to c can be found by taking the first derivative.

$$\frac{\partial F}{\partial c} = \frac{-2b^2 + 2bc}{b^2 a \left(1 - \frac{c^2}{b^2}\right)^{\frac{3}{2}}}$$

Thus, F's extremum comes at c = b. The second derivative is not finite at this point, but since this is the only extremum of F, F is monotonic on both sides of c=b. The two constrained extrema for the interval $0 \leq c \leq b$ will come at c = 0 and c = b. One of which necessarily will be the constrained maximum and the other will be the constrained minimum.

$$F(c = 0) = 1 + \frac{2b}{a}$$

$$F(c = b) = 1 + \frac{2(b-c)}{a \left(1 - c^2 / b^2\right)^{\frac{1}{2}} \Big|_{c=b}}$$

Applying L' Hopital's Rule gives:

$$F(c = b) = 1$$

$$\rightarrow F_{max}(c) = 1 + \frac{2b}{a} \text{ for } 0 \leq c \leq b$$

III.h.2 An Upperbound for the Surface Area Ratio in the Other Case

If x = f:

$$\frac{y^2}{a^2} + \frac{z^2}{b^2} = 1 - \frac{f^2}{a^2}$$

$$\rightarrow S = \pi ab\left(1 - \frac{f^2}{a^2}\right)$$

The area of the membrane is less than that of the ellipse + the circumference times the height a-f.

$$S_m < S_a + C_a(a-f)$$

The circumference of the ellipse is less than the circumference of a rectangle of sides $2y_{max}$ and $2z_{max}$

$$\rightarrow S_m < S_a + 4(a-f)(a+b)(1 - \frac{f^2}{a^2})$$

$$\rightarrow \frac{S_m}{S_a} < 1 + 4\frac{(a-f)(a+b)}{\pi ab(1 - \frac{f^2}{a^2})^{\frac{1}{2}}}$$

Call this bound G. Taking its first derivative gives:

$$\frac{\partial G}{\partial f} = \frac{4a(f-a)(a+b)}{\pi a^3 b(1 - f^2/a^2)^{\frac{3}{2}}}$$

The extremum of G comes at f = a. Unfortunately the second derivative is discontinuous at this point. But f=a is the only extremum of G; therefore, G is monotonic on both sides of f=a. In the range of interest $0 \leq f \leq a$, the constrained extrema will thus occur at f=0 and f=a. One of these will be the constrained maxima; the other the constrained minimum.

$$G(f=0) = 1 + \frac{2(a+b)}{\pi b}$$

Applying L'Hopital's Rule gives:

$$G(f=a) = 1$$

$$\rightarrow G_{max} = 1 + \frac{2(a+b)}{\pi b}$$

III.h.3 The Cellular Configuration that Yields the Largest Induced Membrane Potential

A separation of variables is not possible for general elliptical geometries, so an exact analytic solution is not currently possible. A technique for approximating the potential that is sometimes used is to assume that the membrane's conductivity is zero. This provides boundary conditions which are separable in spheroidal coordinates. [8]

There is justification for assuming negligible conductivity. In general the membrane conductivity might be 10^{-6} - 10^{-8} mho/m, whereas the cytoplasmic and media's conductivity are at 1mho/m.

For this particular application there might even be more of a reason for making such a calculation for V_{max}. When Bernhardt and Pauly used the above approximation they found that the maximum voltage drops occur when the cells have a line of symmetry parallel to the electric field. And they found that this maximum occurs at the line of symmetry. Let's look at an electric field line at this line of symmetry with an area of dA. From steady state solutions it is known that:

$$(\sigma_e + j\omega\varepsilon_e)E_e \cdot dA = (\sigma_m + j\omega\varepsilon_m)E_m \cdot dA = (\sigma_c + j\omega\varepsilon_c)E_c \cdot dA$$

Therefore as σ_m is decreased, E_m would be expected to increase. It

would not be expected to increase by the same proportion as the decrease, since the other parameters would also be affected. But an increase would definitely be expected. Since $V_m = E_m \delta_m$, V_m would also be expected to increase. Therefore, as $\sigma_m \rightarrow 0$ we would expect that V_m might reach a maximum.

Intuition aside, numerical data for several geometries indicates that these approximations are reasonable for intracellular and extracellular electric fields. [16] Thus one would expect it to be valid for the voltage across the membrane as well.

Since it appears the maximum voltage drop occurs when an axis of symmetry is parallel to the imposed electric field [8], the data from Bernhardt and Pauly can be used. For a given height in the direction of the electric field, the highest membrane voltage drop occurred with an oblate spheroid with its small axis in the direction of the electric field.

For cells in monolayer, however, this is a ridiculous model. The shortest axis is perpendicular to the cover glass which is also perpendicular to the electric field. The largest drop for a cell in a reasonable geometry, therefore, is that of a cylinder with its large axis perpendicular to the electric field. Bernhardt and Pauly found this to be the second largest drop.

III.h.4 The Maximum Change in Membrane Potential

Using Laplace's equation and making the same assumptions as for the ac spherical case we get the following solutions to the electric field being applied to a cell with a cylindrical geometry:

$$\phi_1 = -E_o r\cos\theta + \frac{\phi_e}{r}\cos\theta$$

$$\phi_2 = -\phi_{m1} r\cos\theta + \frac{\phi_{m2}}{r}\cos\theta$$

$$\phi_3 = -\phi_c r\cos\theta$$

With boundary conditions of:

$$\sigma_e E^1{}_r(r = R_e) = \sigma_m E^2{}_r(r = R_e)$$

$$\sigma_m E^2{}_r(r = R_c) = \sigma_c E^3{}_r(r = R_c)$$

$$\phi_1(r = R_e) = \phi_2(r = R_e)$$

$$\phi_2(r = R_c) = \phi_3(r = R_c)$$

Thus there are four linear equations for the four unknown parameters:

$$(\sigma_m + j\omega\varepsilon_m)(\phi_{m1} + \frac{\phi_{m2}}{R_e^2}) = (\sigma_e + j\omega\varepsilon_e)(E_o + \frac{\phi_e}{R_e^2})$$

$$(\sigma_c + j\omega\varepsilon_c)\phi_c = (\sigma_m + j\omega\varepsilon_m)(\phi_{m1} + \frac{\phi_{m2}}{R_c^2})$$

$$-E_o R_e + \frac{\phi_e}{R_e} = -\phi_{m1} R_e + \frac{\phi_{m2}}{R_e}$$

$$-\phi_{m1} R_c + \frac{\phi_{m2}}{R_c} = -\phi_c R_c$$

Solving these equations simultaneously and plugging in numbers gives:

$$\Delta V_m = .002m \cdot E_o$$

III.h.5 The Upper Bound for the Intracellular Electric Field

Accumulating the results of the last few sections, the upper bound for the average value of any coordinate component of the electric field is:

$$\frac{\sigma_m V_{max} S_m}{\sigma_c \delta_d S_a} = .002E_o \cdot \max(1 + \frac{2b}{a}, 1 + \frac{2(a+b)}{\pi b})$$

IV. Distortion and Rectification Due to Electrode-Electrolyte Interactions

IV.a Introduction

Relating the applied electric field that the cells perceive to the current and voltage that is applied at the electrodes is very important to interpreting the results of our proline incorporation data. For this reason we have undertaken a study that analyzes the amount of distortion and rectification that occurs in an applied field with respect to its source.

IV.b Background

In the proline experiments an electric field was applied across a region of a chamber by two electrodes placed on either side of the region (Figure 11). For this regional field to be a pure sinusoid, devoid of harmonic distortion or rectification, the applied voltage and current must belong to particular families of solutions. Namely, the applied voltage must possess a certain normalized spectrum, and the applied current must possess a particular normalized spectrum that are solutions to the constraints imposed by the chamber.

· Current in a region is related to the voltage across the region by the expression:

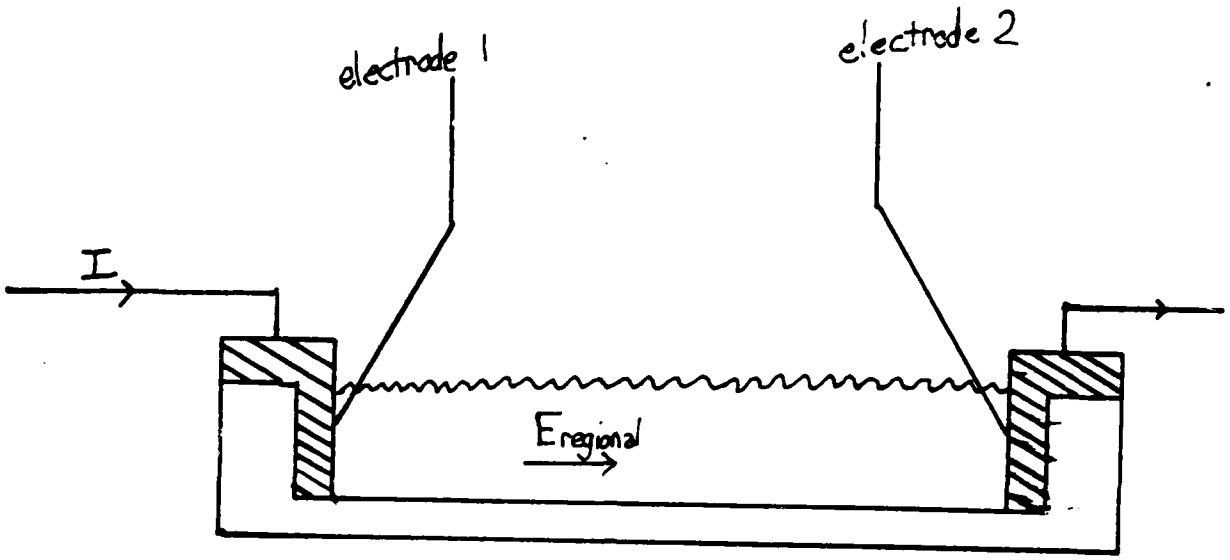

Figure 11

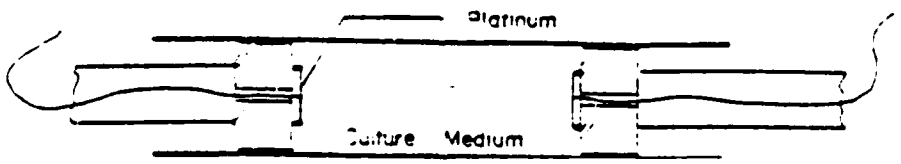

Electrode area = 1.22cm-2.

Figure 12

$$I = Y(V)V$$

where Y is the admittance of the region. By using admittances, charge conservation can be expressed as:

$$\sum I = 0$$

for currents entering a node. From Figure 11 then it can be seen that:

$$I_{applied} = I_{bath}$$

the media in the region can be accurately modeled as having a real, constant conductivity. Then assuming the region's geometry results in a uniform field:

$$E_c = \frac{I_{applied}}{\sigma_c A}$$

$$\frac{I_{applied}}{E_c} = \sigma_c A$$

The ratio of the region's field to the applied current is constant; therefore, they possess the same normalized spectrum. For a purely sinusoidal field, the applied current must be purely sinusoidal.

IV.c Voltage

Ampere's and Faraday's Laws for this electro-quasistatic system can be expressed as:

$$Y_{e1}(V)V_{e1} = Y_c V_c = Y_{e2}(V)V_{e2}$$

$$V_{applied} = V_{e1} + V + V_{e2}$$

for a uniform field:

$$V_c = E_c D$$

therefore,

$$V_{applied} = \left(1 + \frac{Y_c}{Y_{e1}(E_1)} + \frac{Y_c}{Y_{e2}(E_2)}\right) E_c D$$

$$\frac{V_{applied}}{E_c} = \left(1 + \frac{Y_c}{Y_{e1}(E_1)} + \frac{Y_c}{Y_{e2}(E_2)}\right) D$$

Expressions such as the Butler - Volmer Equation and experimental data indicate that $Y_e(E_e)$ is not a constant. Therefore, the ratio is not constant with respect to E. The region's electric field and the applied voltage do not share the same normalized spectrum. A purely sinusoidal applied voltage will not produce a purely sinusoidal E; otherwise, they

would share the same normalized spectrum. sk

To get a purely sinusoidal regional field, one must apply a purely sinusoidal current and a more complicated voltage -- a voltage that has frequency components other than the fundamental. It can be said then that the applied voltage is harmonically distorted. Since it does not possess the same spectrum as a pure sinusoid, it is possible that the applied voltage might also be rectified with respect to the regional field.

IV.d Rectification

If the regional electric field is not rectified with respect to the applied voltage, then in all but the most pathological cases, the regional field must be an odd function of the applied voltage; that is

$$E_c(-V_{applied}) = -E_c(V_{applied}).$$

Since

$$I_c = E_c \sigma_c A = I$$

this condition can equivalently be expressed that I_c must be an odd function of $V_{applied}$,

$$I(V_{applied}) = -I(-V_{applied})$$

Therefore,

$$V_{applied}(I) = -V_{applied}(-I)$$

Since the admittance is a one-to-one mapping of voltage to current, Y(V) can be expressed as Y(I) and Z(I) can be calculated.

$$V_{applied}(I) = Z_{e1}(I)I + Z_{e2}(I)I + Z_c I$$

$$V_{applied}(I) = (Z_{e1}(I) + Z_{e2}(I) + Z_c)I$$

The sum $Z_{e1}(I) + Z_{e2}(I)$ needs to be an even function of I to avoid rectification.

From Figure 11 the current I's positive direction is defined to be the path within the region from electrode 1 to electrode 2. Each electrode can be described as having a characteristic impedance, $Z_{char}(I_{char})$, for current that is defined as positive when flowing from the electrode to the electrolyte. For electrode 1, $I_{char} = I$. For electrode 2, $I_{char} = -I$. Therefore:

$$Z_{e1}(I) + Z_{e2}(I) = Z_{char\text{-}e1}(I) + Z_{char\text{-}e2}(-I)$$

Thus, if the characteristic impedance functions of the two electrodes are the same, this sum will be an even function of I -- no rectification will occur. If they are not the same, then in all but extremely

pathological cases, there will be rectification.

Real electrodes are not likely to have identical impedances. Rectification of the regional field with respect to the applied voltage is expected.

To produce a purely sinusoidal electric field in the chamber's region, a purely sinusoidal current and voltage that is rectified and is not purely sinusoidal must be applied. Under these circumstances, a current source is much better to use than a voltage source. A purely sinusoidal current gives a purely sinusoidal field; a purely sinusoidal voltage gives a harmonically distorted and rectified field.

IV.e Experiments

Due to the previous analysis, distortion and rectification for an applied sinusoidal voltage is expected. As a result of the imperfect nature of current sources, the distortion and rectification of its normalized spectrum is expected. However, these quantities are expected to be less for the current source. We have conducted experiments to quantify the distortion and rectification of the regional electric field for real, sinusoidal current and voltage sources.

The chamber used is shown in Figure 12. It consists of a cut-open 10 cc syringe that is closed by two rubber stoppers at the opposing ends. Each rubber stopper has a circular 1.22 cm^2 electrode attached to it, and each stopper was movable along the main axis of the syringe.

The electrodes were made of bright platinum metal that was buffered with an emory cloth. They were affixed to the stoppers with Epoxy. After which, they were repeatedly washed with a Q-tip soaked in 1N HCl/HNO_3 and wiped with an emory cloth. The emory cloth increased the effective surface area of the electrode and removed most of the epoxy that might have attached to the electrodes.

Media was introduced into the syringe through a small hole that was made in the side of the syringe. Each day media was loaded and removed through the hole.

The experimental configuration is shown in Figure 13. The test resistors were chosen so that the magnitude of the impedance of the resistor corresponded to ten to fifty percent of the magnitude of the path's total impedance. From the previous analysis, it is known that the current through the resistor is linearly related to the electric field in the media. Since current is linearly related to voltage through a resistor, it is known that the voltage across the resistor is linearly related without rectification to the electric field in the media. This voltage then possesses the same normalized spectrum as the electric field in the media -- from it the harmonic distortion and rectification of the media's electric field with respect to a pure sinusoid was determined.

The voltage drop was converted to a digital signal and stored by using an Analog to Digital Converter interfaced to an IBM-XT computer. The frequency spectrum was calculated using the Asyst scientific software package.

IV.f Data

Experimental runs were conducted using two different media: .15M KCl and Dulbecco's Modified Eagle Media (Gibco -- 1X preparation). The voltage source was a Wavetek waveform generator, and the current source was the custom-built current source that was used in our proline incorporation experiments. Both sources are digital generators with high resolution and stable frequency outputs. The Wavetek generator's output was found to not be purely sinusoidal. When the chamber was replaced by a resistor in the configuration of Figure 13, a 0.2% dc offset and a harmonic distortion of less than 2% were found at each of the frequencies and current densities for which the experiment was run. This "background" distortion and rectification was subtracted from each of the stored spectra to yield "corrected" spectra.

The following frequency sinusoids were applied: .1, 1, 10, and 100 Hz. The following peak current densities were applied at each frequency for both sources: .001, .01, .1, 1, 10 mA/cm^2. From the resulting spectra the percent harmonic distortion and rectification were calculated. Percent harmonic distortion was defined as one hundred times the magnitude of the dc component of the corrected and normalized spectrum (normalized with respect to magnitude not intensity). Percentage harmonic distortion was defined as one hundred times the sum of the magnitude of the non-fundamental harmonics of the corrected and normalized spectrum.

The results are plotted in Figures 14-16. Percent rectification was found to decrease with increasing current densities and with increasing frequencies. Percent distortion increased with increasing current densities, but decreased with increasing frequency.

This raised a major question: what is the mechanism of the frequency dependence of the metal-electrode-electrolyte rectification? To explain this, future work will quantitatively examine the specific electrochemical reactions that have rate constants on the order of .1 to 10 seconds.

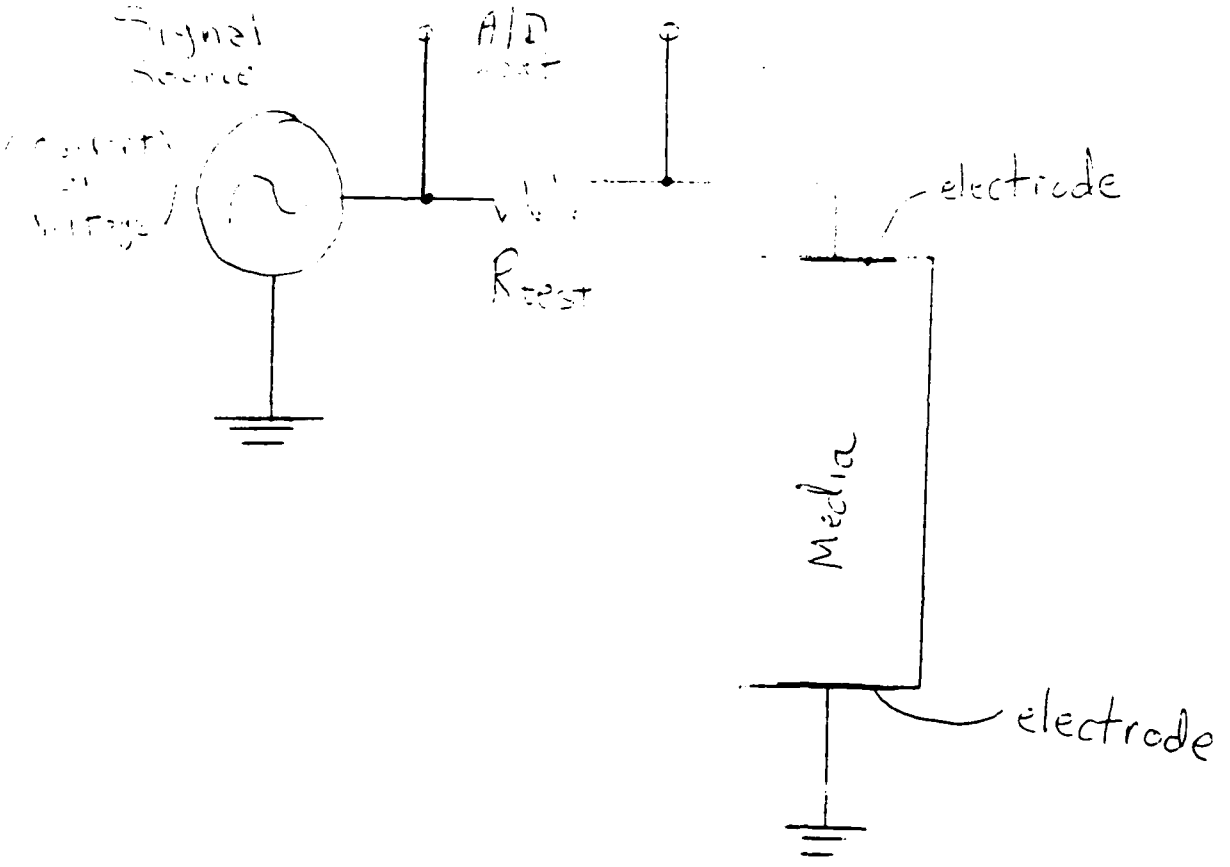

Figure 13

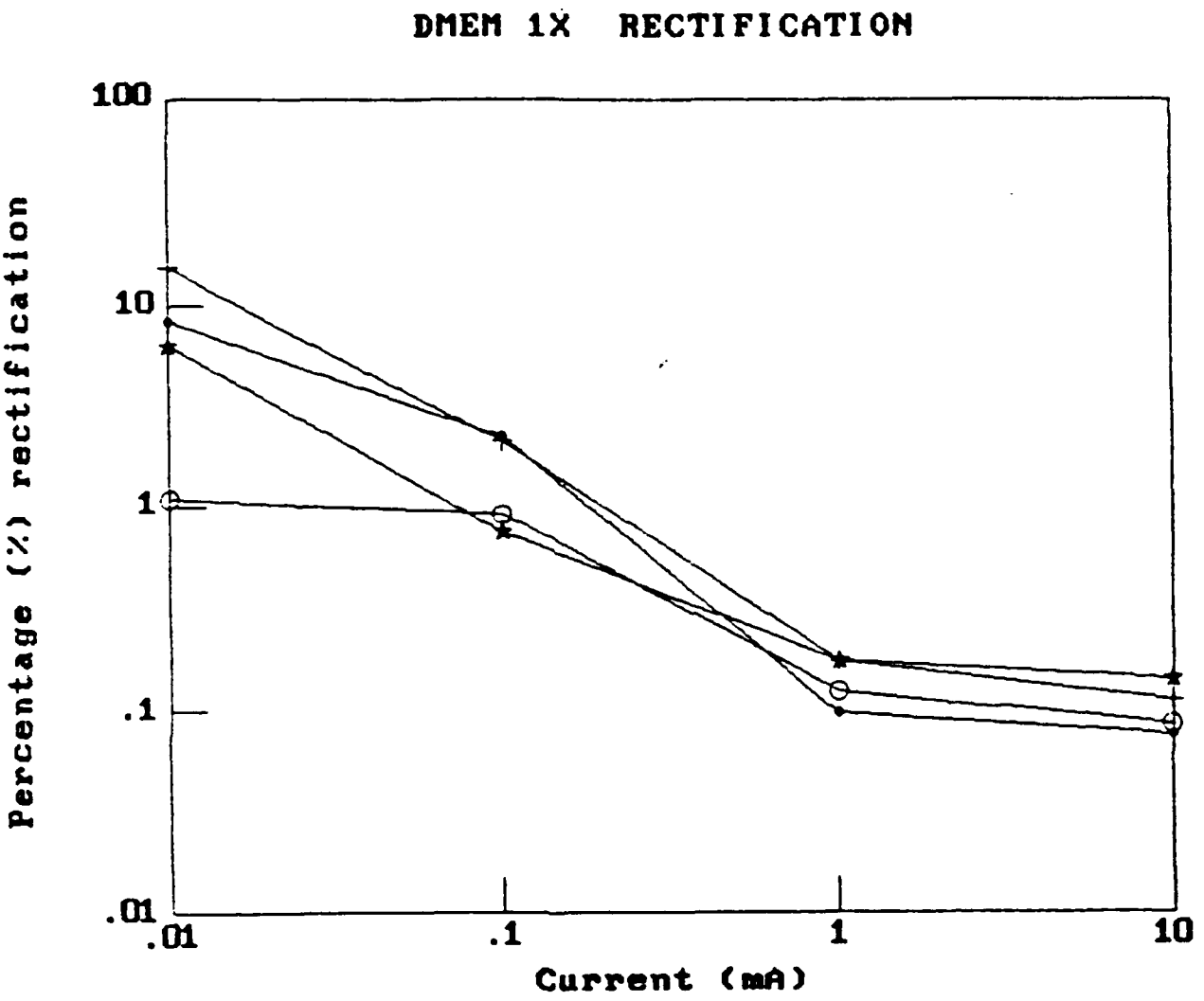

Figure 14

.1 Hz is represented by the circle; 1 Hz by the dot;
10 Hz by the star; and 100 Hz by the cross-bar.

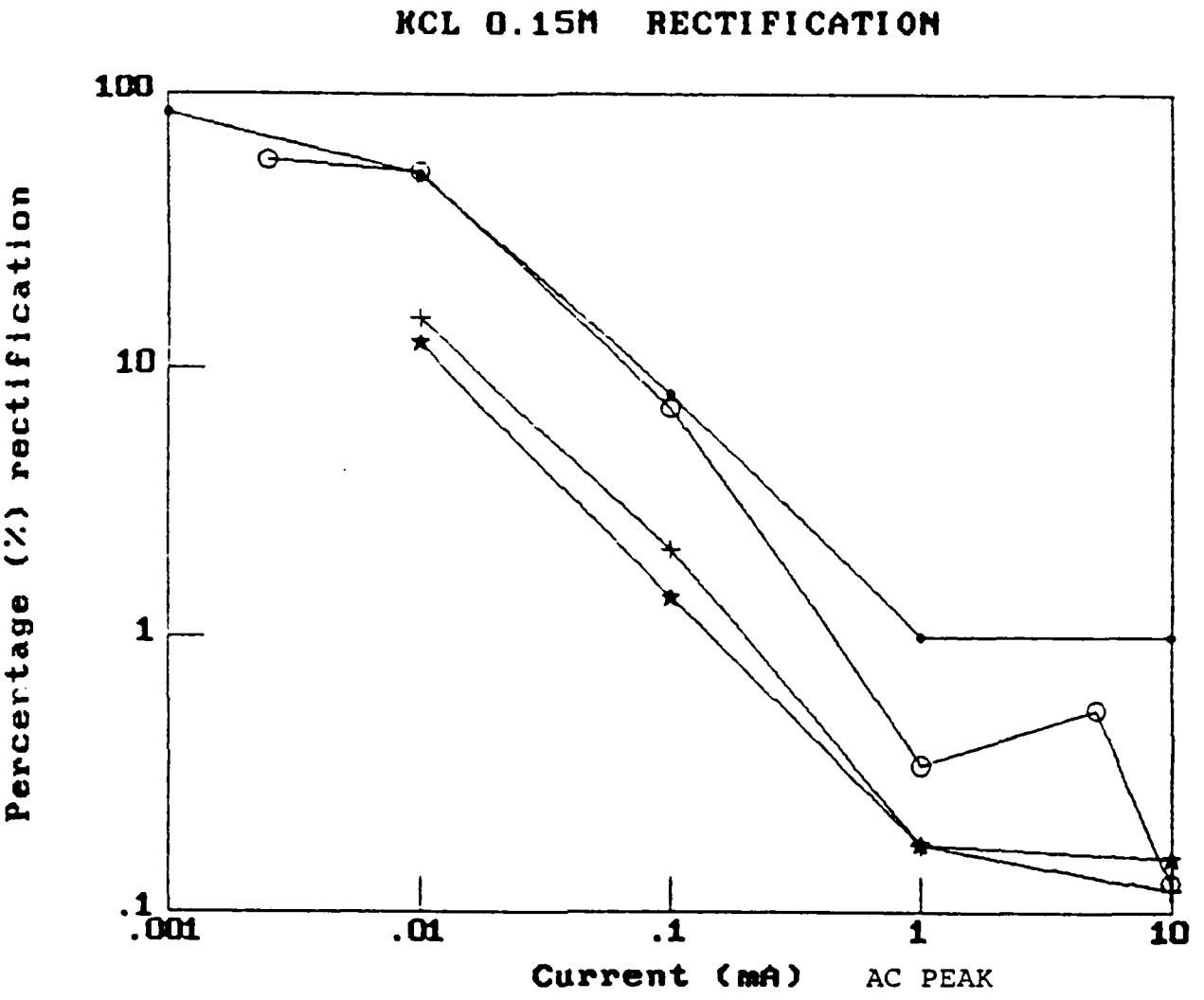

Figure 15

.1 Hz is represented by the circle; 1 Hz by the dot; 10 Hz by the star; and 100 Hz by the cross-bar.

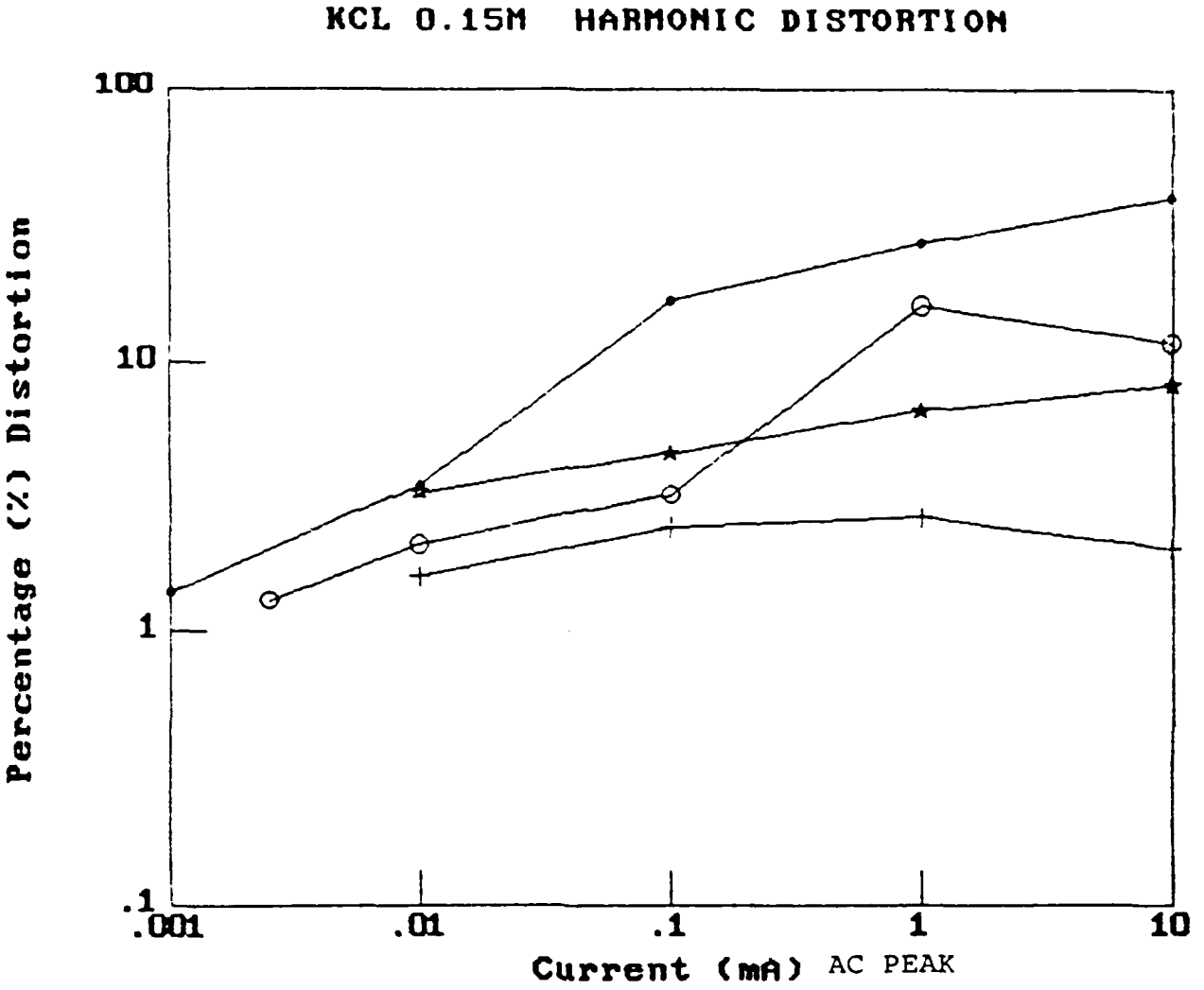

Figure 16

.1 Hz is represented by the circle; 1 Hz by the dot; 10 Hz by the star; and 100 Hz by the cross-bar.

REFERENCES AND NOTES

1. Hall, B.K., p.125, Developmental and Cellular Skeletal Biology , Academic Press, New York (1978).

2. E. Bell, B. Ivarson and C. Merrill, Proc. Nat. Acad. Sci. 76, 1274 (1979).

3. Digestion of the fabricated tissue was carried out by bathing the tissue in 0.2% crude collagenase (Worthington Enzymes, New Jersey) in buffered saline solution for 30-45 minutes. Cells were separated by centrifugation at 1200 rpm for 5 minutes. The cells were lysed with a 0.5% sodium dodecyl sulfate, 10 mM Tris buffer, 1 mM EDTA and 5% BSA solution to release intracellular protein which was then precipitated with 20% TCA with 0.25% tannic acid onto glass filters, ETOH dried. then counted in an LKB scintillation counter. Trypsin (1x, Gibco, Long Island, N.Y.) in divalent cation free buffered saline was used to release cells from monolayer culture.

4. H.P. Ehrlich, et al. Biochem. Med. 28, 273 (1982).

5. This assumes proline to be ≈5.6 times more abundant in collagen than non-collagenase protein.

6. B. Nusgens et al., Collagen Rel. Res. 4,351 (1984)

7. K.J. Mcleod, Ph. D. thesis, Massachusetts Institute of Technology (1986).

8. M. Klee and R. Plonsey, Biophys. J. 12, 1661 (1972).

9. J.J. Tomasek and E.D. Hay, J. Cell Biol. 99, 536 (1984).

10. Bassett, C.A.L., chapter 1, Vol III, The Biochemistry and Physiology of Bone G.H. Bourne (editor), Academic Press, New York, 1971

11. A.J. Kalmijn, Science 218, 916 (1982).

12. Lucifer Yellow is an appropriate dye for monitoring transport due to its membrane impermeability, low molecular weight, and high quantum yield (.25). (W. Stewart, Nature 292:17-21 (1981)).

13. J. Th. G. Overbeek, pp. 194-243, Electrokinetic phenomena, in Colloid Science I , H.R. Kruyt ed., Elsevier Publishing Company, Amsterdam, 1952.

14. Bernhardt and Pauly list 10μm as the average size radius for mammals. Human fibroblasts are considerably large, however, so 30μm appears to be more appropriate.

15. The speed of light in aqueous media is $7.025 \cdot 10^7$ (m/s). Thus, it takes 35ps for an electromagnetic wave to penetrate 2.5mm, the length of a long fibroblast. This amount of time corresponds to a frequency of 28GHz. Electrostatics will thus hold for any frequency much below this.

16. J. Bernhardt and H. Pauly, Biophysik 10, 89-98 (1973).

17. Admittances account for dp/dt in the charge conservation expression.

END

12-86

DTIC